

TRANSACTIONS OF THE
INSTITUTE OF
MEASUREMENT & CONTROL

Original Manuscript - Control

Disturbance-observer-based attitude control under input nonlinearity

Transactions of the Institute of
Measurement and Control
1–10

© The Author(s) 2021



Article reuse guidelines:

sagepub.com/journals-permissions

DOI: 10.1177/0142331221997204

journals.sagepub.com/home/timUmair Javid¹ and Hongyang Dong² 

Abstract

A disturbance observer-based control scheme is proposed in this paper to deal with the attitude stabilization problems of spacecraft subjected to external disturbances, parameter uncertainties, and input nonlinearities. Particularly, the proposed approach addresses the dead-zone issue, a non-smooth nonlinearity affiliated with control input that significantly increases controller design difficulties. A novel nonlinear disturbance observer (NDO) is developed, which relaxes the strong assumption in conventional NDO design that disturbances should be constants or varying with slow rates. After that, a special integral sliding mode controller (ISMC) is combined with the NDO to achieve asymptotic convergence of system states. Simulations are performed in the presence of time-varying disturbances, parameter uncertainties, and dead-zone nonlinearity to justify the effectiveness of the proposed control scheme.

Keywords

Attitude control, input nonlinearity, dead zone, sliding mode control, disturbance observer

Introduction

The attitude stabilization problems have gained extensive attention over the years, due to their significance in space mission and widespread applications. Many practical issues, such as external disturbances, parameter modeling uncertainties, and input nonlinearities, must be considered in attitude controller design. To this end, many research results have been proposed to solve attitude stabilization problems using different control techniques, such as back-stepping control (Kristiansen et al., 2009), passivity-based control (Gui and Vukovich, 2016; Ulrich et al., 2016), and adaptive control (Reza Alipour et al., 2018; Wen et al., 2018). In particular, sliding mode control (SMC) (Cui et al., 2017) techniques have been used extensively due to their multiple advantages, including inherent robustness and easy-to-implement structure (Zhang and Zheng, 2014; Zhang et al., 2014).

SMC is known for its robustness against system uncertainties and external disturbances. It uses discontinuous feedback control action to force the system trajectories to reach the pre-designed sliding manifolds. However, discontinuity can lead to the chattering problem, which is undesirable from a practical engineering viewpoint. Though this can be avoided by replacing the discontinuous term in controller with the sigmoid approximation function (Saghafinia et al., 2015), such approximation may result in deterioration of controller performance. Also, SMC can not attenuate mismatched uncertainties and disturbances unless combined with other robust techniques (Shtessel et al., 2014). Recently, integral sliding mode controller (ISMC) method has attracted wide research interest due to its ability to mitigate the chattering issue

(Liang et al., 2012; Xu et al., 2014; Zhang et al., 2016). This technique provides an extra degree of freedom to devise an appropriate control law for the system (Comanescu et al., 2008). A first-order ISMC was proposed for attitude tracking problems in Pukdeboon and Zinober (2012). A second-order ISMC framework was developed in Tiwari et al. (2015).

External disturbances and parameter uncertainties are common and inevitable issues that can hinder the successful completion of space missions. For this reason, the spacecraft attitude control law must be able to handle external disturbance and parameter uncertainties (Lu et al., 2013; Wu et al., 2011). High-gain switching functions can be used to overcome the effect of system parameter uncertainties but may result in input chattering. An adaptive SMC was employed for attitude tracking control problems subjected to external disturbances in Reza Alipour et al. (2018). Disturbance observer-based control methods have been proposed in many studies (Chen and Ge, 2015; Ginoya et al., 2014; Hu et al., 2014; Pukdeboon and Siricharuanun, 2014; Sofyali et al., 2018; Zhang et al., 2018), in which disturbance estimates are incorporated with control laws to reject the disturbances directly. Such control schemes can also mitigate input chattering and approximately

¹College of Automation Engineering, Nanjing University of Aeronautics and Astronautics, China

²School of Engineering, University of Warwick, UK

Corresponding author:

Hongyang Dong, School of Engineering, University of Warwick, Gibbet Road, Coventry, CV4 7AL, UK.

Email: Hongyang.Dong@warwick.ac.uk

compensate parameter uncertainties, therefore improving overall control performance. The disturbance and parameter vibrations in flexible spacecraft were compensated using a disturbance observer in Liu et al. (2018). A disturbance observer was designed and combined with the controller for control allocation improvement in Qiao et al. (2018). A composite control law that employs extended state observer (ESO) and an additive controller was developed to remove external disturbance in Chen et al. (2018). Another ESO-based control laws were presented in Ye et al. (2017) and Li et al. (2016) for formation flying of spacecraft. Back-stepping was combined with the observer to formulate a stabilization control scheme in Sun and Zheng (2017). An iterative learning-based observer was combined with fault-tolerant control for spacecraft stabilization control in Hu et al. (2018).

Input nonlinearity is another important practical issue that originates from the physical constraints of control actuators. For example, the dead-zone nonlinearity is encountered when reaction wheels are used as actuators in spacecraft attitude control (Hu et al., 2008). However, most of the control schemes ignore the input nonlinearity such as dead-zone and saturation. Such design may lead to system performance degradation or sometimes even destabilization, causing mission failure (Pang and Yang, 2013). The input nonlinearity, along with the external disturbances and parameter uncertainties, can significantly increase the difficulty of control system design. Though some controllers had been proposed in recent years (Chen et al., 2018; Lu et al., 2013) to deal with attitude control problems subject to input saturation, those results are difficult to be extended to handle dead-zone problems, where the actual input is a nonlinear function of friction. The attitude stabilization problem for an uncertain system with dead-zone was solved using SMC in Hu et al. (2008), but strict upper bounds on disturbances were required. Variable structure control was combined with the adaptive control to deal with the input dead-zone in Hu (2007) and Yan et al. (2005). However, over-adaptation and parameter drift are serious concerns in those studies.

The difficulty of attitude control problems with dead zones stems from the fact that the factors affecting dead zones and their parameters are partially or totally unknown. The presence of dead zones severely limits the control system performance and influences the dynamic characteristics of closed-loop system. Therefore, control techniques that are robust to the dead zone, in addition to external disturbance and system uncertainty, are of vital importance for spacecraft attitude control. In this paper, a novel observer-based attitude stabilization control method is developed to address this challenging problem. A new nonlinear disturbance observer (NDO) is designed to estimate the system's combined disturbance, composed of time-vary external disturbances, system uncertainties, and dead zone. The key features of the proposed NDO include finite-time convergence and relaxation of strong assumptions related to the bounds of uncertainties. These features enable the proposed NDO to estimate various classes of disturbances. After that, the NDO is integrated with ISMC to achieve attitude stabilization. Lyapunov's stability theory is employed to analyze the convergence of estimation error and the closed-loop system's stability. The developed NDO-ISMC structure ensures asymptotic convergence of system states

while reducing the control input chattering significantly. Comparative simulations are performed to justify presented theoretical results and show the control performance of our controller.

The remainder of this paper is arranged as follows. First, Section II describes the system dynamics. After that, the control problem is formulated in Section III. In Section IV, our NDO is designed to obtain the combined disturbance estimate. The composite control law is formulated using ISMC and NDO. Simulation results with brief discussions are presented in section IV. Finally, some conclusive remarks are given in Section VI.

Spacecraft attitude model

The attitude model of a rigid-body spacecraft is provided in this section. The case of a fully-actuated system is considered here.

Attitude kinematics and dynamics

The quaternion representation-based model is used for attitude control of spacecraft in this work. Assume an Euler angle $\phi(t) \in R$ is given about a particular Euler axis $\hat{e} = [\hat{e}_1 \ \hat{e}_2 \ \hat{e}_3]^T \in R^3$, then the corresponding quaternion Q can be described as

$$Q = \begin{bmatrix} \hat{e} \sin(\phi) \\ \cos(\phi) \end{bmatrix} = \begin{bmatrix} \Omega_v \\ \Omega_4 \end{bmatrix} \quad (1)$$

where $\Omega_v = [\Omega_1 \ \Omega_2 \ \Omega_3]^T$ is the vector part of Q , and Ω_4 is the scalar part of Q . The quaternion Q can also be defined by $Q = [\Omega_1 \ \Omega_2 \ \Omega_3 \ \Omega_4]^T$, and it satisfies

$$\Omega_1^2 + \Omega_2^2 + \Omega_3^2 + \Omega_4^2 = 1 \quad (2)$$

The rigid-body spacecraft attitude kinematics are given as Hu (2007)

$$\dot{\Omega}_v = \frac{1}{2}(\Omega_4 I_3 + \Omega_v \times) \omega \quad (3)$$

$$\dot{\Omega}_4 = -\frac{1}{2} \Omega_v^T \omega \quad (4)$$

where $\omega = [\omega_1 \ \omega_2 \ \omega_3]^T$ is the angular velocity in body reference frame B with respect to inertial reference frame I . The notion $\Omega_v \times$ for vector Ω_v is employed to denote the corresponding skew-symmetric matrix defined as follows

$$\Omega_v \times = \begin{bmatrix} 0 & -\Omega_3 & \Omega_2 \\ \Omega_3 & 0 & -\Omega_1 \\ -\Omega_2 & \Omega_1 & 0 \end{bmatrix} \in R^{3 \times 3} \quad (5)$$

In addition, the rigid-body dynamics are given as Hu (2007)

$$J \dot{\omega} = -\omega \times J \omega + u(t) + d(t) \quad (6)$$

where parameter $u(t) = [u_1(t) \ u_2(t) \ u_3(t)]^T \in R^3$ is the control input, $d(t) = [d_1(t) \ d_2(t) \ d_3(t)]^T \in R^3$ is the time-varying external disturbance and $J \in R^{3 \times 3}$ represents the inertia matrix.

Assumption 1. The inertia matrix J is time-dependent and has the form $J(t) = J_0 + \Delta J(t)$. Here J_0 is a constant nonsingular matrix, and $\Delta J(t)$ represents the time-varying uncertainties. Additionally, $\Delta J(t)$ is a differentiable function for all $t > 0$. For ease of expression, $J(t)$ and $\Delta J(t)$ are denoted as J and ΔJ , respectively, in the remainder of this paper.

Assumption 2. For the given rigid-body spacecraft, time-varying external disturbance $d(t)$ and inertial uncertainty ΔJ are bounded by unknown positive constants, that is, $\|d(t)\| \leq \pi_1$ and $\|\Delta J\| \leq \pi_2$.

Remark 1. In general, the inertia matrix of a spacecraft is measured before launch and used in attitude control. However, it can change by many reasons like the fuel consumption and structure variation (Kim et al., 2010). The mathematical expression related to the changes in inertia caused by some specific factors can be described, such as the consumption of propellant. But changes due to many other factors are unknown; for example, the movement of peripheral devices installed on spacecraft. Therefore, it is reasonable to consider ΔJ as unknown and time-varying.

Problem formulation

In this section, the dead-zone model used in this paper is presented, and a transformed attitude model is deduced for a rigid-body spacecraft.

Dead zone

The dead zone is one of the most consequential nonlinearities encountered in spacecraft actuators and can severely limit the system performance. It is usually time-varying with unknown parameters. We describe the dead zone for an output vector $u(t) = [u_1, u_2, u_3, \dots, u_n]^T$ and an input vector $v(t) = [v_1, v_2, v_3, \dots, v_n]^T$ as follows

$$u_i(t) = \mathcal{DZ}(v_i(t)) = \begin{cases} m_i(v_i(t) - b_u), & \text{for } v_i(t) \geq b_u \\ 0, & \text{for } b_l < v_i(t) < b_u \\ m_i(v_i(t) - b_l), & \text{for } v_i(t) \leq b_l \end{cases} \quad (7)$$

where $m_i > 0$, $b_u > 0$ and $b_l < 0$ are dead-zone parameters.

The expression in equation (7) can be reorganized as

$$u_i(t) = \mathcal{DZ}(v_i(t)) = m_i v_i(t) + \eta(v_i(t)) \quad (8)$$

and here $\eta(v_i(t))$ follows

$$\eta(v(t)) = \begin{cases} -m_i b_u, & \text{for } v_i(t) \geq b_u \\ -m_i v(t), & \text{for } b_l < v_i(t) < b_u \\ -m_i b_l, & \text{for } v_i(t) \leq b_l \end{cases} \quad (9)$$

Then, we use the following equation to denote the vector-form dead-zone projection, which is the direct extension of equation (8)

$$u(t) = \mathcal{DZ}(v(t)) = m v(t) + \eta(v(t)) \quad (10)$$

where $m = \text{diag}[m_i]$ is the dead-zone slope.

Assumption 3. The essential attributes of the actuator dead-zone considered in the paper are as follows:

- (1) The dead-zone output $u(t)$ is not available for measurement.
- (2) The parameters b_u , b_l and m_i are unknown. However, the sign of parameters are known i.e. $b_u > 0$, $b_l < 0$ and $m_i > 0$.
- (3) The dead-zone parameter are bounded by unknown constants, that is, $b_u \in [b_{u,\min}, b_{u,\max}]$, $b_l \in [b_{l,\min}, b_{l,\max}]$ and $m_i \in [m_{\min}, m_{\max}]$. Here, $b_{l,\min}$, $b_{l,\max}$, $b_{u,\min}$, $b_{u,\max}$, m_{\max} and m_{\min} are known constants.

From the key features (1) and (2) in the Assumption 3, one has $\eta(v(t))$ bounded, that is

$$|\eta(v(t))| \leq \rho \quad (11)$$

where the unknown upper bound ρ satisfies

$$\rho = \max\{m_{\max} b_{u,\max} - m_{\max} b_{l,\min}\} \quad (12)$$

Remark 2. The attribute (1) in assumption 3 is common for all practical systems. Features (2) and (3) are also commonly adopted in the literature (Lewis et al., 1999; Wang et al., 2004).

System transformation

In this section, input nonlinearities are introduced in system dynamics, and transformations are performed based on Assumption 1, to facilitate the NDO design. Employing Assumption 1 and equation (6), we have

$$(J_0 + \Delta J)\dot{\omega} = -\omega \times (J_0 + \Delta J)\omega + u(t) + d(t)$$

$$J_0\dot{\omega} + \Delta J\dot{\omega} = -\omega \times J_0\omega + u(t) - \omega \times \Delta J\omega + d(t)$$

$$J_0\dot{\omega} = -\omega \times J_0\omega + u(t) + d(t) - \omega \times \Delta J\omega - \Delta J\dot{\omega}$$

Using equation (6) with algebraic simplification results in

$$J_0\dot{\omega} = -\Delta J J^{-1}[-\omega \times J\omega + u(t) + d(t)] - \omega \times J_0\omega - \omega \times \Delta J\omega + u(t) + d(t)$$

$$\begin{aligned} \dot{\omega} &= J_0^{-1}[-\Delta J J^{-1}[u(t) - \omega \times J\omega + d(t)]] + J_0^{-1}d(t) + J_0^{-1}u(t) \\ &\quad - J_0^{-1}[\omega \times J_0\omega + \omega \times \Delta J\omega] \\ &= J_0^{-1}\{-\omega \times \Delta J\omega - \Delta J J^{-1}[u(t) - \omega \times J\omega]\} + J_0^{-1}u \\ &\quad + J_0^{-1}[I_3 - \Delta J J^{-1}]d - J_0^{-1}\omega \times J_0\omega \end{aligned} \quad (13)$$

A compact form of $\dot{\omega}$ can be written as

$$\dot{\omega} = \mathcal{F} + \mathcal{M} + b u \quad (14)$$

where $\mathcal{M} = J_0^{-1}\{-\omega \times \Delta J\omega - \Delta J J^{-1}[u(t) - \omega \times J\omega]\} + J_0^{-1}[I_3 - \Delta J J^{-1}]d$, $\mathcal{F} = -J_0^{-1}\omega \times J_0\omega$ and $b = J_0^{-1}$.

Introducing the dead-zone expression in equation (10) into equation (14), one has

$$\begin{aligned}
\dot{\omega} &= \mathcal{F} + \mathcal{M} + b[\mathcal{D}\mathcal{Z}(v(t))] \\
&= \mathcal{F} + \mathcal{M} + b[mv(t) + \eta(v(t))] \\
&= \mathcal{F} + \mathcal{M} + bmv(t) + b\eta(v(t))
\end{aligned} \tag{15}$$

By defining $D = \mathcal{M} + b\eta(v(t))$, equation (15) is equivalent to

$$\dot{\omega} = \mathcal{F} + bmv(t) + D \tag{16}$$

Remark 3. The combined disturbance D consists of the effect of external disturbance, parameter uncertainties, and dead-zone nonlinearity.

Problem statement

This paper aims to develop a stabilization controller for the spacecraft attitude control problem subjected to dead zone, parameter uncertainties and external disturbances, formalized by

$$\lim_{t \rightarrow \infty} (\omega) = 0, \quad \lim_{t \rightarrow \infty} (\Omega_v) = 0, \quad \lim_{t \rightarrow \infty} (\Omega_4) = 1 \tag{17}$$

Before designing our control strategy, the following definition and lemma regarding finite-time convergence are presented as preliminary results.

Definition 1. Bhat and Bernstein (2000). Consider the nonlinear system

$$\dot{y} = f(y), \quad f(0) = 0, \quad y \in R^n \tag{18}$$

where the function $f(y) : d \rightarrow R^n$ is continuous on the neighborhood of $y = 0$. Equilibrium point $y = 0$ of the system in equation (18) is finite time (FT) convergent provided the following statements hold true, (a) asymptotically stable in U , here U is an open neighborhood of the origin and $U \subseteq d$. (b) FT convergent in U , that is, for all $y \in [U, 0)$ there exist settling time (T_s). Such that, every possible solution of (18) that can be defined with $y(t, y_0) \in [U, 0), \forall t = [0, T_s]$ satisfy $\lim_{t \rightarrow T_s} (y) = 0$.

Lemma 1. Bhat and Bernstein (2000). For the nonlinear system (18), there exist variables $0 < \alpha < 1$ and $\lambda > 0$, along with a continuous Lyapunov function $V(y)$ such that they satisfy

$$\dot{V}(y) + \lambda[V(y)]^\alpha \leq 0 \tag{19}$$

Then, the system is FT stable if $V(y)$ is unbounded and time T_e needed to reach equilibrium point is given by

$$T_e \leq \frac{V(y_0)^{1-\alpha}}{\lambda(1-\alpha)} \tag{20}$$

Disturbance observer and controller design

In this section, a NDO is developed along with an ISMC law to realize the aforementioned attitude control objective.

Rigorous stability analysis of the proposed observer and control law is provided.

Disturbance observer design

We aim to design a NDO to estimate the unknown combined disturbance $D(t)$ and therefore make compensation and enhance the closed-loop control performance. Our design is described as follows

$$\begin{cases} \hat{d} &= \zeta + p(\omega) \\ \dot{\zeta} &= -L(\omega)[\hat{d}] + L(\omega)[-F - bmv(t)] \\ p(\omega) &= \left[\frac{\partial p(\omega)}{\partial \omega} \right] \dot{\omega} = L(\omega)\dot{\omega} \end{cases} \tag{21}$$

where \hat{d} denotes the estimate of D and $L(\omega) = \frac{\partial p(\omega)}{\partial \omega}$.

Theorem 1. For the attitude dynamics of spacecraft in equation (6), the transformed dynamics in equation (16), and the designed NDO in equation (21). The estimation error $d_e = D - \hat{d}$ converges to a neighborhood of zero in FT, and its convergence path is constrained by the following inequalities

$$\|d_e(t)\| \leq \begin{cases} \sqrt{2V_1(0)}e^{-L(\omega)t} & \dot{D} = 0 \\ \sqrt{2V(0)}e^{-2(1-\beta)L(\omega)t} + \frac{2\eta}{\sqrt{\beta L(\omega)}} & \dot{D} \neq 0 \text{ and } |\dot{D}| \leq \eta \end{cases} \tag{22}$$

Proof. The disturbance observer error is defined as

$$\begin{aligned} d_e &= D - \hat{d} \\ \dot{d}_e &= \dot{D} - \dot{\zeta} - \dot{p}(\omega) \end{aligned} \tag{23}$$

Using the observer design in equation (21), we have

$$\begin{aligned} \dot{d}_e &= \dot{D} + L(\omega)\{\mathcal{F} + bmv(t) + p(\omega)\} - \left[\frac{\partial p(\omega)}{\partial \omega} \right] \dot{\omega} \\ &= \dot{D} + L(\omega)\{\zeta\} + L(\omega)\{\mathcal{F} + bmv(t) + p(\omega)\} \\ &\quad - L(\omega)\{\mathcal{F} + bmv(t) + D\} \\ &= \dot{D} - L(\omega)d_e \end{aligned} \tag{24}$$

Consider the Lyapunov function

$$\begin{aligned} V_1 &= \frac{1}{2}d_e^T d_e \\ \dot{V}_1 &= d_e^T \dot{d}_e \\ &= d_e^T \dot{D} - d_e^T L(\omega)d_e \end{aligned} \tag{25}$$

Further analysis is divided into the subsequent two cases.

Case 1. When $\dot{D} = 0$, one has

$$\dot{V}_1 = -L(\omega)d_e^T d_e \leq -2L(\omega)V_1 \tag{26}$$

The solution to equation (26) is $V_1 \leq V_1(0) \exp^{-2L(\omega)t}$ and the d_e satisfies

$$\|d_e(t)\| \leq \sqrt{2V_1(0)}e^{-L(\omega)t} \tag{27}$$

Case 2. When $\dot{D} \neq 0$ and $\|\dot{D}\| \leq \eta$, one has

$$\begin{aligned}
\dot{V}_1 &\leq \|d_e\|\eta - L(\omega)\|d_e\|^2 \\
&\leq -L(\omega)\|d_e\|^2 + \eta^2 \\
&\leq -L(\omega)\|d_e\|^2 - \beta L(\omega)\|d_e\|^2 + \beta L(\omega)\|d_e\|^2 + \eta^2 \\
&\leq -(1-\beta)L(\omega)\|d_e\|^2 - \beta L(\omega)\|d_e\|^2 + \eta^2
\end{aligned}$$

where the constant β is selected as $0.5 < \beta < 1$. Based on the above analysis, one has

$$\dot{V}_1 \leq -2(1-\beta)L(\omega)V, \quad \forall \|d_e\| \geq \frac{2\eta}{\sqrt{\beta L(\omega)}} \quad (28)$$

By equation (28), one can further show that

$$\dot{V}_1 \leq V_1(0)e^{-2(1-\beta)L(\omega)t}, \quad \forall \|d_e\| \geq \frac{2\eta}{\sqrt{\beta L(\omega)}} \quad (29)$$

$$\|d_e(t)\| \leq \sqrt{2V(0)}e^{-2(1-\beta)L(\omega)t} + \frac{2\eta}{\sqrt{\beta L(\omega)}} \quad t \geq 0 \quad (30)$$

From equation (26) and (28), it is evident that the observer estimation error converges to zero, that is, $d_3 \rightarrow 0$. Furthermore, the convergence trajectory of estimation error is given by equation (27) and (30). These complete the proof.

Remark 4. From equations (27) and (30), one can see that the convergence rate of estimation error is dependent on η and β . Larger values of η and β results in smaller estimation error and can lead to a faster convergence rate. However, chattering will be induced if too large parameter values are selected.

Remark 5. In the literature (Chen and Ge, 2015; Hu et al., 2014; Sun and Zheng, 2017), the specific values of the upper bounds of disturbances are required to design observers. This strong and impractical requirement is relaxed in our design.

ISMC controller design

In this section, an ISMC scheme is developed and integrated with the NDO. The sliding surface to formulate ISMC law is defined as follows

$$\sigma = \omega + k_s \Omega_v + \int_0^t \phi d\tau \quad (31)$$

where $1 > k_s > 0$ and ϕ is designed by

$$\phi = C_1 \omega + C_2 \Omega_v - k_s \dot{\Omega}_v \quad (32)$$

and here $C_1 > 0$ and $C_2 > 0$ are positive constants. Initial value of function $\phi(0)$ is set to be $\phi(0) = -[\omega(0) + k_s q_v(0)]$ so that $s(0) = 0$.

Taking derivative of the sliding surface, one has

$$\begin{aligned}
\dot{\sigma} &= \dot{\omega} + k \dot{\Omega}_v + \phi \\
&= \dot{\omega} + k \dot{\Omega}_v + C_1 \omega + C_2 \Omega_v - k_s \dot{\Omega}_v \\
&= \dot{\omega} + C_1 \omega + C_2 \Omega_v \\
&= \mathcal{F} + bm v(t) + D + C_1 \omega + C_2 \Omega_v
\end{aligned} \quad (33)$$

The proposed control law has the following form

$$v(t) = v_{eq}(t) + v_s(t) \quad (34)$$

$$v_{eq}(t) = (bm)^{-1}[-\mathcal{F} - C_1 \omega - C_2 \Omega_v - \hat{d}] \quad (35)$$

$$v_s(t) = -(bm)^{-1}[P\sigma + Qsat(\sigma)] \quad (36)$$

where $P = diag[p_i]$ and $Q = diag[q_i]$ with $p_i > 0$ and $q_i > 0$. The saturation function $sat(\sigma_i)$ satisfies $sat(\sigma_i) = [sat(\sigma_1), sat(\sigma_2), sat(\sigma_3), \dots, sat(\sigma_i)]^T$ with

$$sat(\sigma_i) \begin{cases} sign(\sigma_i), & \text{if } |\sigma_i| > \epsilon_i \\ \frac{\sigma_i}{\epsilon_i}, & \text{if } |\sigma_i| \leq \epsilon_i \end{cases} \quad (37)$$

where $\epsilon_i > 0$ defines the thickness of the sliding surface boundary layer. Based on equations (33) and (34), one has

$$\begin{aligned}
\dot{\sigma} &= [-\hat{D} - P\sigma - Qsat(\sigma)] + D \\
\dot{\sigma} &= d_e - P\sigma - Qsat(\sigma)
\end{aligned} \quad (38)$$

Then, the following theorem summarizes the development of our control law and the closed-loop system stability.

Theorem 2. Considering the attitude model described in equation (6) and the NDO designed in equation (21). Then the controller in equation (34) compels the system states to approach the sliding surface as defined in equation (31) and ultimately converge to zero.

Proof. Considering the following Lyapunov function

$$V = \frac{1}{2} \sigma^T \sigma + V_1 \quad (39)$$

$$\dot{V} = \sigma^T d_e - \sigma^T P\sigma - \sigma^T Qsat(\sigma) + \dot{V}_1 \quad (40)$$

Similar to Theorem 1, we split the analysis into the following two cases.

Case 1. When $\dot{D} = 0$ and $\dot{V}_1 = -L(\omega)\|d_e\|^2$, one has

$$\begin{aligned}
\dot{V} &\leq \|\sigma\| \|d_e\| - P\|\sigma\|^2 - L(\omega)\|d_e\|^2 - |\sigma|Qsat(\sigma) \\
&\leq \|\sigma\| \|d_e\| - P\|\sigma\|^2 - L(\omega)\|d_e\|^2 + \frac{\|\sigma\|^2}{4L(\omega)} - \frac{\|\sigma\|^2}{4L(\omega)} \\
&\quad - |\sigma|Qsat(\sigma) \\
&\leq -\left(P - \frac{1}{4L(\omega)}\right)\|\sigma\|^2 - \left(\sqrt{L(\omega)}\|d_e\| - \frac{\|\sigma\|}{2\sqrt{L(\omega)}}\right)^2 \\
&\quad - |\sigma|Qsat(\sigma)
\end{aligned} \quad (41)$$

Case 2. When $\dot{D} \neq 0$ and $\dot{V}_1 = -(1-\beta)L(\omega)\|d_e\|^2$, $\forall \|d_e\| \geq \frac{\eta}{\sqrt{\beta L(\omega)}}$ with $0 < \beta < 1$, one has

$$\begin{aligned}
\dot{V} &\leq \|\sigma\| \|d_e\| - P\|\sigma\|^2 - (1-\beta)L(\omega)\|d_e\|^2 - |\sigma|Q_{sat}(\sigma) \\
&\leq \|\sigma\| \|d_e\| - (1-\beta)L(\omega)\|d_e\|^2 + \frac{\|\sigma\|^2}{4(1-\beta)L(\omega)} \\
&\quad - \frac{\|\sigma\|^2}{4(1-\beta)L(\omega)} \\
&\quad - P\|\sigma\|^2 - |\sigma|Q_{sat}(\sigma) \\
&\leq - \left(\sqrt{(1-\beta)L(\omega)}\|d_e\| - \frac{\|\sigma\|}{2\sqrt{(1-\beta)L(\omega)}} \right)^2 \\
&\quad - \left(P - \frac{1}{4(1-\beta)L(\omega)} \right) \|\sigma\|^2 \\
&\quad - |\sigma|Q_{sat}(\sigma)
\end{aligned} \tag{42}$$

It should be noted that the fact: $\sigma^T Q_{sat}(\sigma) = \sum_{i=1}^n Q_i \sigma_i \text{sat}(\sigma_i) \geq 0$ is employed in these inequalities.

Equations (41) and (42) are satisfied for all $P - \frac{1}{4L(\omega)} > 0$ and $\epsilon_i > 0$, i.e., $\dot{V} \leq 0$. Hence, the closed-loop system is proved stable asymptotically, completing the whole proof.

Remark 6. A major concern of SMC is the chattering problem. To alleviate this issue, the saturation function $\text{sat}(\sigma_i)$ in equation (37) is employed in our design. The parameter ϵ_i determines the switching threshold and helps to decrease the chattering phenomenon.

Simulation results and discussion

In this section, the performance of the developed NDO-ISMIC control scheme is tested by numerical simulations. Comparative simulation results, along with detailed discussions, are presented to demonstrate the effectiveness of our method.

The attitude model of a rigid-body spacecraft is adapt from Chen et al. (2018). The nominal value of the inertia matrix and the time-varying uncertain inertia of spacecraft are given as follows

$$J_0 = \begin{bmatrix} 20 & 1.2 & 0.9 \\ 1.2 & 17 & 1.4 \\ 0.9 & 1.4 & 15 \end{bmatrix} \text{Kg.m}^2$$

$$\Delta J = \text{diag}([\sin(0.1t) \quad 2\sin(0.2t) \quad \sin(0.3t)]) \text{Kg.m}^2$$

Furthermore, the external disturbance used in simulations is selected as

$$d(t) = 0.05[\sin(0.1t) \quad \sin(0.2t) \quad \sin(0.3t)]^T \text{N.m}$$

The initial value of attitude quaternion is opted as $Q(0) = [0.3, -0.2, -0.3, -0.8832]^T$, and the initial angular velocity is selected as $\omega(0) = [0, 0, 0]^T$ rad/s.

The constant parameters used to simulate the dead-zone nonlinearity, the NDO, and the proposed NDO-ISMIC law are given in Table 1. Specifically, the parameters K_s, C_1, C_2 construct the sliding surface and can be obtained using Hurwitz criteria. Larger values of C_1 and C_2 will result in larger control input. The parameters P and Q are used to tune chattering in control input and keep system states on the sliding surface. A too-large value of P will destabilize the system,

Table 1. Control parameters for numerical simulations.

	Parameters
Dead-zone	$m_l = 1, b_u = 0.05, b_l = -0.06,$ $b_{l,min} = -0.07, m_u = 1.25, m_l = 0.85,$ $b_{l,max} = -0.01, b_{u,min} = 0.01, b_{u,max} = 0.07,$
NDO-ISMIC law	$\zeta(0) = [0, 0, 0]^T, a_0 = 1.5, s = 3, \eta = 0.8$ $K_s = 0.75, C_1 = 1.2, C_2 = 0.02, \epsilon_i = 0.01$ $P = 6.5, Q = 0.01$
AISMIC law	$C_1 = 1.2, C_2 = 0.02, k = 40.5, \gamma = 0.01,$ $a_2 = 10, a_1 = 0.01, \hat{L} = 0$

and smaller values will lead to a sluggish response. The parameter ϵ_i determines the saturation function. The larger value of ϵ_i does not mean a fast convergence rate. However, smaller values result in the chattering phenomenon.

Proper selection of the NDO design parameters enables the convergence of estimates to actual disturbance. In this work, $p(w)$ and $L(w)$ are take as

$$\begin{aligned}
p(w) &= a_0 J_0 \left[\omega + \frac{\omega^s}{s!} \right] \\
L(w) &= a_0 J_0 \text{diag} \left(\left[1 + \omega_1^{s-1}, 1 + \omega_2^{s-1}, 1 + \omega_3^{s-1} \right] \right)
\end{aligned} \tag{43}$$

where the constant parameters a_0 and s are given in Table 1. It is found through simulations that the convergence time of the estimation error decreases with an increase of a_0 .

Spacecraft stabilization controller using an adaptive ISMC (AISMIC) subjected to dead zone, external disturbance, and parameter uncertainties is simulated for comparison. The AISMIC follows

$$\begin{aligned}
v(t) &= v_{eq}(t) + v_s(t) \\
v_{eq}(t) &= (bm)^{-1} [-\mathcal{F} - C_1 \omega - C_2 \Omega_v] \\
v_s(t) &= -k \text{sign}(\sigma(t)^\gamma - \hat{L} \text{sign}(\sigma(t)))
\end{aligned} \tag{44}$$

where parameters C_1 and C_2, k and γ are provided in Table 1. The parameter \hat{L} is obtained using adaptive law, given by

$$\dot{\hat{L}} = a_2 (\|\sigma(t)\| - a_1 * \hat{L}) \tag{45}$$

the parameter values of the constants $a_2, a_1,$ and \hat{L} are selected as given in Table 1.

The simulation results of the proposed NDO are depicted in Figure 1. One can observe that the disturbance estimate converges to the actual value after 80 sec. The effect of lumped disturbance is reduced by using NDO through feed-forward compensation. The convergence of disturbance estimation error with time is shown in Figure 2.

Spacecraft attitude orientation is given in Figure 3. Note that the attitude quaternion coincides to the equilibrium point in 100 s. It can be observed that attitude quaternion reaches the equilibrium position in a similar fashion under NDO-ISMIC and AISMIC. The trajectories for the angular velocities of the rigid-body spacecraft are given in Figure 4, and they converge in 100 s. Angular velocities are more smooth for the proposed controller during steady-state operations as shown in Figure 4(a) and Figure 4(b). Additionally, it is evident that the angular velocities have less overshoot under NDO-ISMIC

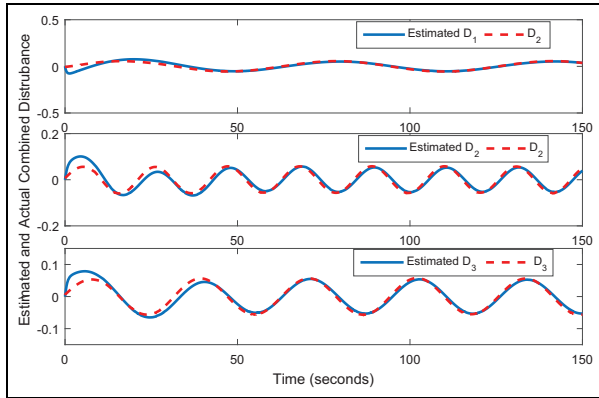


Figure 1. Estimates and estimation errors of the combined disturbance.

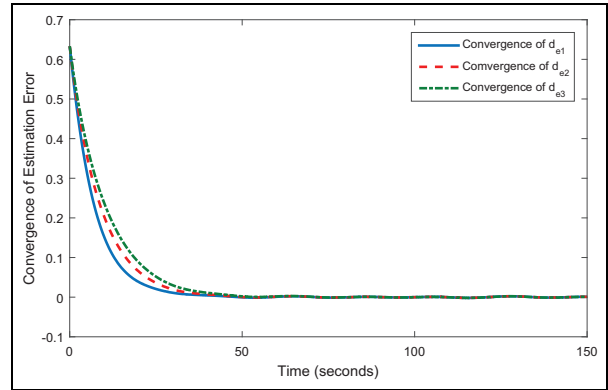


Figure 2. Convergence property of disturbance estimation error.

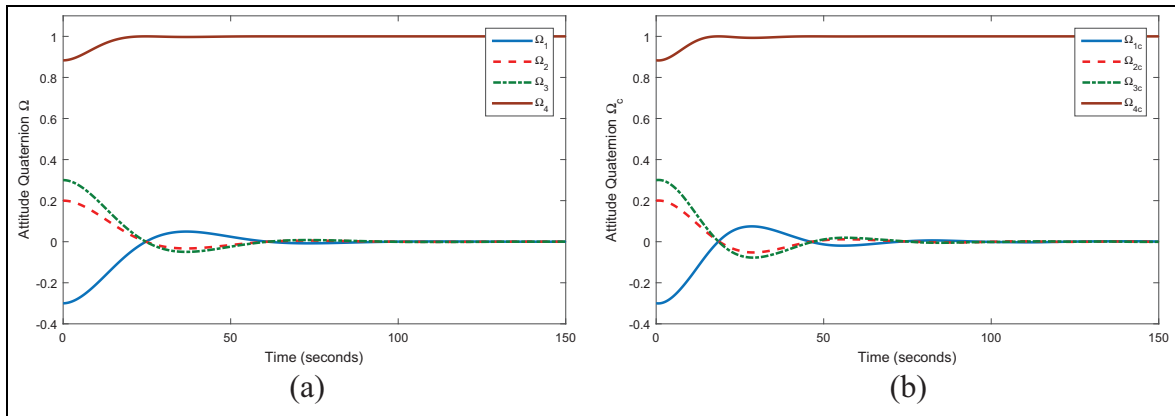


Figure 3. Attitude quaternion error response: (a) Proposed NDO-ISMC law; (b) AISMC law.

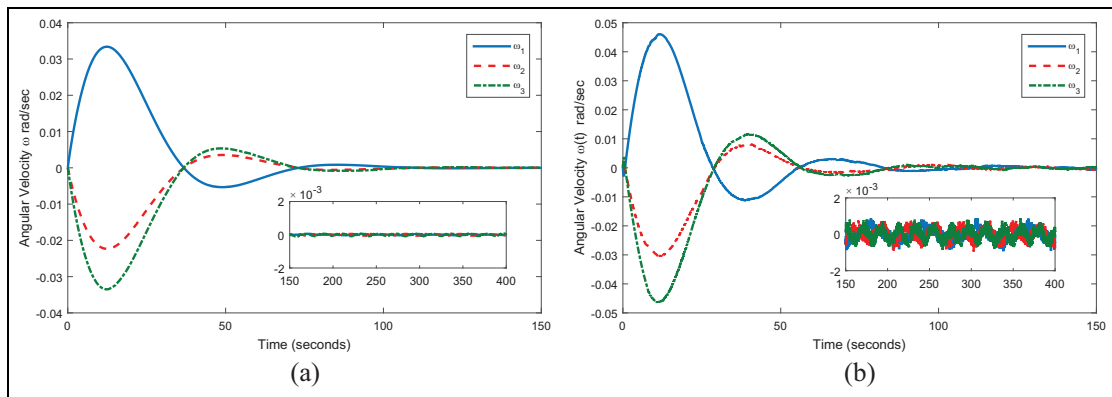


Figure 4. Angular velocity evolution: (a) Proposed NDO-ISMC law; (b) AISMC law.

when compared with AISMC. The sliding surfaces for both the controllers are shown in Figure 5. It is clear from the figure that there is no reaching phase, and system states are on the sliding surface from the start under our NDO-ISMC. However, the sliding surface for AISMC is not

smooth and diverges from zero occasionally, which can result in controller performance degradation. A possible cause of the divergence of the sliding surface from the equilibrium point is the presence of non-smooth input uncertainty in the system.

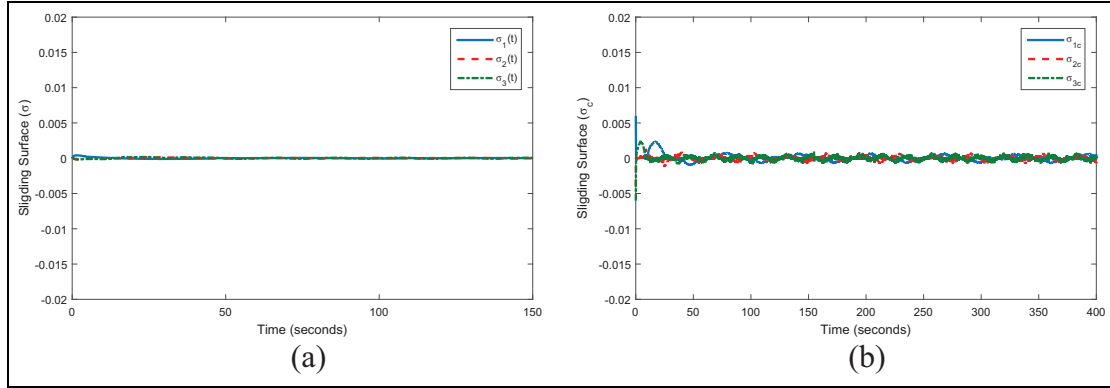


Figure 5. Sliding surface: (a) NDO-based ISMC law; (b) ASMC law.

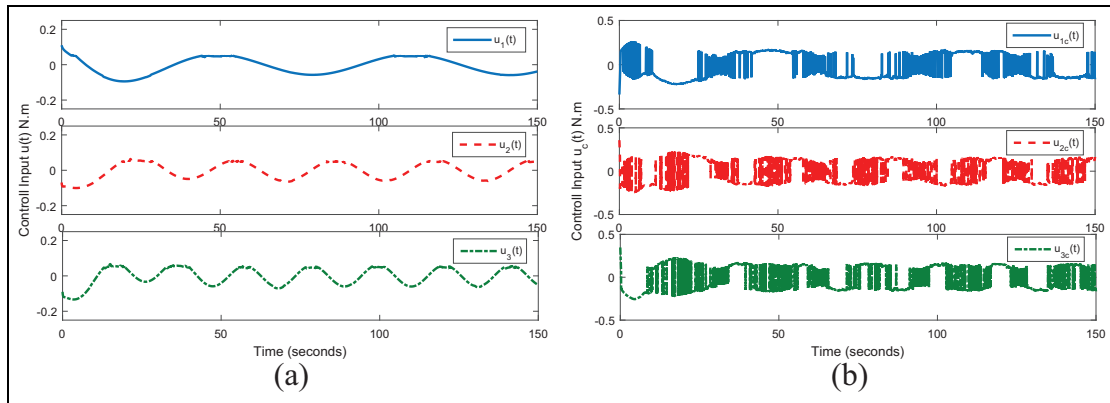


Figure 6. Control input torque: (a) NDO-based ISMC law; (b) AISMC law.

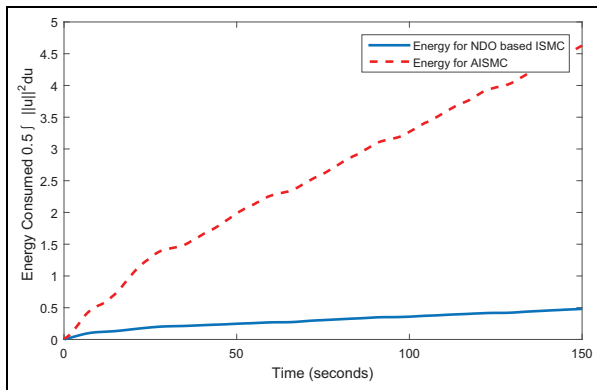


Figure 7. Energy consumption for proposed controller and AISMC law.

The evolution of control input to stabilize the spacecraft system is presented in Figure 6. It is apparent that the control input of NDO-ISMC is smooth and chattering free, in spite of the presence of dead-zone. However, the control input under AISMC law encounters the chattering problem.

Energy consumption for the control laws is shown in Figure 7. The energy for the given control law is calculated using $E = \frac{1}{2} \int_0^t \|u\|^2 du$. The proposed NDO-ISMC control scheme is energy efficient comparatively. The simulation results and subsequent discussion show that the proposed NDO-ISMC control scheme is substantially robust to external disturbances, parameter uncertainties, and input nonlinearities. Furthermore, it is energy efficient, alleviates controller output chattering, and gives better control performance.

Conclusion


A composite control scheme for attitude stabilization of rigid-body spacecraft subjected to external disturbances, parameter uncertainties, and input nonlinearity has been developed. A new NDO was designed to estimate the combined disturbance of the closed-system. The condition for convergence of the designed NDO was rigorously established. Notably, the changing rate of the combined disturbance was not required to be zero or almost zero. Hence, the proposed NDO is able to handle a wide range of disturbances. Simulation results showed that the proposed NDO-ISMC method efficiently

achieved attitude control objective in the presence of non-smooth dead zone, external disturbances, and parameter uncertainties.

Declaration of conflicting interests

The author(s) declared no potential conflicts of interest with respect to the research, authorship, and/or publication of this article.

ORCID iD

Hongyang Dong  <https://orcid.org/0000-0003-4302-5323>

References

- Bhat SP and Bernstein DS (2000) Finite-time stability of continuous autonomous systems. *SIAM Journal on Control and Optimization* 38(3): 751–766.
- Chen H, Song S and Zhu Z (2018) Robust finite-time attitude tracking control of rigid spacecraft under actuator saturation. *International Journal of Control, Automation and Systems* 16(1): 1–15.
- Chen M and Ge SS (2015) Adaptive neural output feedback control of uncertain nonlinear systems with unknown hysteresis using disturbance observer. *IEEE Transactions on Industrial Electronics* 62(12): 7706–7716.
- Comanescu M, Xu L and Batzel TD (2008) Decoupled current control of sensorless induction-motor drives by integral sliding mode. *IEEE Transactions on Industrial Electronics* 55(11): 3836–3845.
- Cui R, Chen L, Yang C and Chen M (2017) Extended state observer-based integral sliding mode control for an underwater robot with unknown disturbances and uncertain nonlinearities. *IEEE Transactions on Industrial Electronics* 64(8): 6785–6795.
- Ginoya D, Shendge PD and Phadke SB (2014) Sliding mode control for mismatched uncertain systems using an extended disturbance observer. *IEEE Transactions on Industrial Electronics* 61(4): 1983–1992.
- Gui H and Vukovich G (2016) Finite-time output-feedback position and attitude tracking of a rigid body. *Automatica* 74: 270–278.
- Hu Q (2007) Variable structure output feedback control of a spacecraft under input dead-zone non-linearity. *Proceedings of the Institution of Mechanical Engineers, Part G: Journal of Aerospace Engineering* 221(2): 289–303.
- Hu Q, Li B and Qi J (2014) Disturbance observer based finite-time attitude control for rigid spacecraft under input saturation. *Aerospace Science and Technology* 39: 13–21.
- Hu Q, Ma G and Xie L (2008) Robust and adaptive variable structure output feedback control of uncertain systems with input non-linearity. *Automatica* 44(2): 552–559.
- Hu Q, Niu G and Wang C (2018) Spacecraft attitude fault-tolerant control based on iterative learning observer and control allocation. *Aerospace Science and Technology* 75: 245–253.
- Kim DH, Choi DG and Oh HS (2010) Inertia Estimation of Spacecraft Based on Modified Law of Conservation of Angular Momentum. *Journal of Astronomy and Space Sciences* 27(4): 353–357.
- Kristiansen R, Nicklasson P and Gravdahl J (2009) Satellite attitude control by quaternion-based backstepping. *IEEE Transactions on Control Systems Technology* 17(1): 227–232.
- Lewis FL, Tim WK, Wang LZ and Li ZX (1999) Deadzone compensation in motion control systems using adaptive fuzzy logic control. *IEEE Transactions on Control Systems Technology* 7(6): 731–742.
- Li B, Hu Q and Ma G (2016) Extended state observer based robust attitude control of spacecraft with input saturation. *Aerospace Science and Technology* 50: 173–182.
- Liang YW, Ting LW and Lin LG (2012) Study of Reliable Control Via an Integral-Type Sliding Mode Control Scheme. *IEEE Transactions on Industrial Electronics* 59(8): 3062–3068.
- Liu Z, Liu J and Wang L (2018) Disturbance observer based attitude control for flexible spacecraft with input magnitude and rate constraints. *Aerospace Science and Technology* 72: 486–492.
- Lu K, Xia Y and Fu M (2013) Controller design for rigid spacecraft attitude tracking with actuator saturation. *Information Sciences* 220: 343–366.
- Pang H and Yang X (2013) Robust optimal sliding-mode tracking control for a class of uncertain nonlinear MIMO systems. *Journal of Applied Mathematics* 2013(1): 1–9.
- Pukdeboon C and Siricharuanun P (2014) Nonsingular terminal sliding mode based finite-time control for spacecraft attitude tracking. *International Journal of Control, Automation and Systems* 12(3): 530–540.
- Pukdeboon C and Zinober A (2012) Control Lyapunov function optimal sliding mode controllers for attitude tracking of spacecraft. *Journal of the Franklin Institute* 349(2): 456–475.
- Qiao J, Liu Z and Li W (2018) Anti-disturbance attitude control of combined spacecraft with enhanced control allocation scheme. *Chinese Journal of Aeronautics* 31(8): 1741–1751.
- Reza Alipour M, Fani Saberi F and Kabgarian M (2018) Modelling, design and experimental implementation of non-linear attitude tracking with disturbance compensation using adaptive-sliding control based on quaternion algebra. *Aeronautical Journal* 122(1247): 148–171.
- Saghafinia A, Ping HW, Uddin MN, et al. (2015) Adaptive fuzzy sliding-mode control into chattering free IM drive. *IEEE Transactions on Industry Applications* 51(1): 692–701.
- Shtessel Y, Edwards C, Fridman L and Levant A (2014) *Sliding Mode Control and Observation, Control Engineering*, volume 10. New York, NY: Springer New York.
- Sofyalı A, Jafarov EM and Wisniewski R (2018) Robust and global attitude stabilization of magnetically actuated spacecraft through sliding mode. *Aerospace Science and Technology* 76: 91–104.
- Sun L and Zheng Z (2017) Disturbance-observer-based robust backstepping attitude stabilization of spacecraft under input saturation and measurement uncertainty. *IEEE Transactions on Industrial Electronics* 64(10): 7994–8002.
- Tiwari PM, Janardhanan S and Un Nabi M (2015) Rigid spacecraft attitude control using adaptive integral second order sliding mode. *Aerospace Science and Technology* 42: 50–57.
- Ulrich S, Saenz-Otero A and Barkana I (2016) Passivity-based adaptive control of robotic spacecraft for proximity operations under uncertainties. *Journal of Guidance, Control, and Dynamics* 39(6): 1444–1453.
- Wang XS, Su CY and Hong H (2004) Robust adaptive control of a class of nonlinear systems with unknown dead-zone. *Automatica* 40(3): 407–413.
- Wen H, Yue X and Yuan J (2018) Dynamic scaling-based noncertainty-equivalent adaptive spacecraft attitude tracking control. *Journal of Aerospace Engineering* 31(2): 04017098.
- Wu S, Radice G, Gao Y and Sun Z (2011) Quaternion-based finite time control for spacecraft attitude tracking. *Acta Astronautica* 69(1–2): 48–58.
- Xu JX, Guo ZQ and Lee TH (2014) Design and implementation of integral sliding-mode control on an underactuated two-wheeled mobile robot. *IEEE Transactions on Industrial Electronics* 61(7): 3671–3681.

- Yan JJ, Shyu KK and Lin JS (2005) Adaptive variable structure control for uncertain chaotic systems containing dead-zone nonlinearity. *Chaos, Solitons & Fractals* 25(2): 347–355.
- Ye D, Zhang J and Sun Z (2017) Extended state observer-based finite-time controller design for coupled spacecraft formation with actuator saturation. *Advances in Mechanical Engineering* 9(4): 1–13.
- Zhang C, Wang J, Zhang D and Shao X (2018) Learning observer based and event-triggered control to spacecraft against actuator faults. *Aerospace Science and Technology* 78: 522–530.
- Zhang J and Zheng WX (2014) Design of adaptive sliding mode controllers for linear systems via output feedback. *IEEE Transactions on Industrial Electronics* 61(7): 3553–3562.
- Zhang J, Feng G and Xia Y (2014) Design of estimator-based sliding-mode output-feedback controllers for discrete-time systems. *IEEE Transactions on Industrial Electronics* 61(5): 2432–2440.
- Zhang J, Liu X, Xia Y, Zuo Z and Wang Y (2016) Disturbance observer-based integral sliding-mode control for systems with mismatched disturbances. *IEEE Transactions on Industrial Electronics* 63(11): 7040–7048.